Article

Kinetics and Mechanism of N Hydrogenation in Bis(cyclopentadienyl) Zirconium Complexes and Dinitrogen Functionalization by 1,2-Addition of a Saturated C–H Bond

Wesley H. Bernskoetter, Emil Lobkovsky, and Paul J. Chirik

J. Am. Chem. Soc., **2005**, 127 (40), 14051-14061• DOI: 10.1021/ja0538841 • Publication Date (Web): 17 September 2005

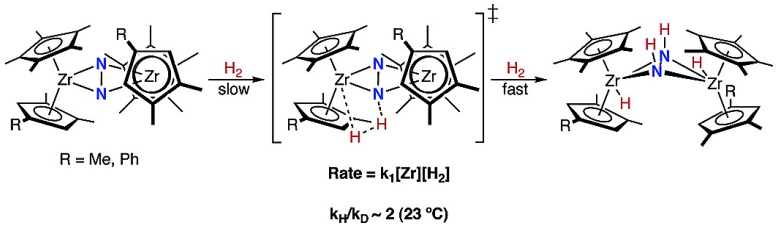

More About This Article

Additional resources and features associated with this article are available within the HTML version:

- Supporting Information
- Links to the 15 articles that cite this article, as of the time of this article download
- Access to high resolution figures
- Links to articles and content related to this article
- Copyright permission to reproduce figures and/or text from this article

View the Full Text HTML

J|A|C|S
ARTICLES
Published on Web 09/17/2005

Kinetics and Mechanism of N_2 Hydrogenation in Bis(cyclopentadienyl) Zirconium Complexes and Dinitrogen Functionalization by 1,2-Addition of a Saturated C−H Bond

Wesley H. Bernskoetter, Emil Lobkovsky, and Paul J. Chirik*

Contribution from the Department of Chemistry and Chemical Biology, Baker Laboratory, Cornell University, Ithaca, New York 14853

Received June 13, 2005; E-mail: pc92@cornell.edu

Abstract: The rates of hydrogenation of the N_2 ligand in the side-on bound dinitrogen compounds, $[(\eta^5\text{-}C_5Me_4H)_2Zr]_2(\mu_2,\eta^2,\eta^2\text{-}N_2)$ and $[(\eta^5\text{-}C_5Me_5)(\eta^5\text{-}C_5H_2\text{-}1,2\text{-}Me_2\text{-}4\text{-}R)Zr]_2(\mu_2,\eta^2,\eta^2\text{-}N_2)$ (R = Me, Ph), to afford the corresponding hydrido zirconocene diazenido complexes have been measured by electronic spectroscopy. Determination of the rate law for the hydrogenation of $[(\eta^5\text{-}C_5Me_5)(\eta^5\text{-}C_5H_2\text{-}1,2,4\text{-}Me_3)Zr]_2(\mu_2,\eta^2,\eta^2\text{-}N_2)$ establishes an overall second-order reaction, first order with respect to each reagent. These data, in combination with a normal, primary kinetic isotope effect of 2.2(1) for H_2 versus D_2 addition, establish the first H_2 addition as the rate-determining step in N_2 hydrogenation. Kinetic isotope effects of similar direction and magnitude have also been measured for hydrogenation (deuteration) of the two other zirconocene dinitrogen complexes. Measuring the rate constants for the hydrogenation of $[(\eta^5\text{-}C_5Me_5)(\eta^5\text{-}C_5H_2\text{-}1,2,4\text{-}Me_3)Zr]_2(\mu_2,\eta^2,\eta^2\text{-}N_2)$ over a 40 °C temperature range provided activation parameters of $\Delta H^{\ddagger} = 8.4(8)$ kcal/mol and $\Delta S^{\ddagger} = -33(4)$ eu. The entropy of activation is consistent with an ordered four-centered transition structure, where H_2 undergoes formal 1,2-addition to a zirconium−nitrogen bond with considerable multiple bond character. Support for this hypothesis stems from the observation of N_2 functionalization by C−H activation of a cyclopentadienyl methyl substituent in the mixed ring dinitrogen complexes, $[(\eta^5\text{-}C_5Me_5)(\eta^5\text{-}C_5H_2\text{-}1,2\text{-}Me_2\text{-}4\text{-}R)Zr]_2(\mu_2,\eta^2,\eta^2\text{-}N_2)$ (R = Me, Ph), to afford cyclometalated zirconocene diazenido derivatives.

Introduction

The global dependence on both bioavailable and synthetic ammonia makes elucidation of the mechanisms of nitrogen fixation of considerable importance.[1] Since Haber's synthesis of ammonia from its constituent elements,[2] chemists have sought a fundamental understanding of how N_2 and H_2 combine to form N−H bonds. Such insight may provide the foundation for new, energy-efficient nitrogen fixation schemes. While considerable progress has been made in understanding the process of N_2 reduction both in the nitrogenase family of enzymes[3,4] and in industrial catalysts,[5] the challenges associated with making spectroscopic measurements on complex biomolecules and metal surfaces have limited mechanistic studies.

The advent of well-defined transition metal complexes that coordinate and functionalize dinitrogen offers the opportunity to elucidate the mechanisms and possibly establish structure−reactivity relationships for N−H bond formation. Molybdenum and tungsten complexes have been useful in providing a fundamental understanding of N_2 coordination[6] and cleavage,[7] and compounds that promote N−H, N−C, and N−heteroatom bond formation have been known for some time.[8] Evolution of the "Chatt-cycle",[9] N_2 functionalization by successive proton and electron transfers, has allowed catalytic ammonia production with single-site molybdenum compounds.[10,11] Significantly, many of the catalytically relevant intermediates have also been identified.[12] Stoichiometric variants of this chemistry have also been extended to iron[13] with the goal of developing efficient biomimetic catalysts.[14]

(1) Smil, V. *Enriching the Earth: Fritz Haber, Carl Bosch, and the Transformation of World Food Production*, MIT Press: Cambridge, MA, 2001.
(2) Haber, F.; van Oordt, G. *Z. Anorg. Chem.* **1905**, *47*, 42.
(3) (a) Dos Santos, P. C.; Igarashi, R. Y.; Lee, H. I.; Hoffman, B. M.; Seefeldt, L. C.; Dean, D. R. *Acc. Chem. Res.* **2005**, *38*, 208. (b) Eady, R. R. *Chem. Rev.* **1996**, *96*, 3013. (c) Burgess, B. K.; Lowe, D. J. *Chem. Rev.* **1996**, *96*, 2983.
(4) For recent mechanistic investigations into substrate binding in nitrogenase enzymes, see: (a) Igarashi, R. Y.; Laryukhin, M.; Dos Santos, P. C.; Lee, H. I.; Dean, D. R.; Seefeldt, L. C.; Hoffman, B. M. *J. Am. Chem. Soc.* **2005**, *127*, 6231. (b) Lee, H. I.; Igarashi, R. Y.; Laryukhin, M.; Doan, P. E.; Dos Santos, P. C.; Dean, D. R.; Seefeldt, L. C.; Hoffman, B. M. *J. Am. Chem. Soc.* **2004**, *126*, 9563.
(5) Ertl, G. *Chem. Rec.* **2001**, 33.
(6) Chatt, J.; Dilworth, J. R.; Richards, R. L. *Chem. Rev.* **1978**, *78*, 589.
(7) (a) LaPlaza, C. E.; Cummins, C. C. *Science* **1995**, *268*, 861. (b) LaPlaza, C. E.; Johnson, A. R.; Cummins, C. C. *J. Am. Chem. Soc.* **1996**, *118*, 709. (c) Solari, E.; DaSilva, C.; Iacono, B.; Hesschenbrouck, J.; Rizzoli, C.; Scopelliti, R.; Floriani, C. *Angew. Chem., Int. Ed.* **2001**, *40*, 3907.
(8) Hidai, M.; Mizobe, Y. *Can. J. Chem.* **2005**, *83*, 358.
(9) Chatt, J.; Pearman, A. J.; Richards, R. L. *Nature* **1975**, *253*, 39.
(10) (a) Ritleng, V.; Yandulov, D. V.; Weare, W. W.; Schrock, R. R.; Hock, A. S.; Davis, W. M. *J. Am. Chem. Soc.* **2004**, *126*, 6150. (b) Yandulov, D. V.; Schrock, R. R. *Science* **2003**, *76*, 301.
(11) Schrock, R. R. *Chem. Commun.* **2003**, 2389.
(12) (a) Yandulov, D. V.; Schrock, R. R. *Inorg. Chem.* **2005**, *44*, 1103. (b) Yandulov, D. V.; Schrock, R. R. *J. Am. Chem. Soc.* **2002**, *124*, 6252.
(13) Betley, T. A.; Peters, J. C. *J. Am. Chem. Soc.* **2003**, *125*, 10782.
(14) (a) Holland, P. L. *Can. J. Chem.* **2005**, *83*, 296. (b) Holland, P. L. In *Comprehensive Coordination Chemistry 2*; McCleverty, J., Meyer, T. J., Eds.; Elsevier: Oxford, 2003; Vol. 8, p 569.

With respect to N_2 hydrogenation, Fryzuk has reported a bis(phosphine)diamido-ligated zirconium dinitrogen complex, $[(P_2N_2)Zr]_2(\mu_2,\eta^2,\eta^2\text{-}N_2)$ (P_2N_2 = PhP($CH_2SiMe_2NSiMe_2CH_2$)$_2$-PPh), that undergoes addition of 1 equiv of dihydrogen, resulting in one new N−H bond and a bridging zirconium hydride.[15,16] Computational studies on the related model complex, $[(p_2n_2)Zr]_2(\mu_2, \eta^2, \eta^2\text{-}N_2)$ (p_2n_2 = $(PH_3)_2(NH_2)_2$), establish that the hydrogenation reaction proceeds through an ordered, four-centered transition structure, where the Zr−H and N−H bonds are formed simultaneously.[17] Subsequent DFT calculations have predicted the addition of a second equivalent of H_2 to have a slightly lower kinetic barrier than the first, but is not observed experimentally owing to the facility of the reverse reaction.[18]

Recently, our laboratory has described a side-on bound zirconocene dinitrogen complex, $[(\eta^5\text{-}C_5Me_4H)_2Zr]_2(\mu_2,\eta^2,\eta^2\text{-}N_2)$ (**1-N$_2$**), that undergoes addition of 2 equiv of H_2 to furnish the hydrido zirconocene diazenido complex, $[(\eta^5\text{-}C_5Me_4H)_2ZrH]_2(\mu_2,\eta^2,\eta^2\text{-}N_2H_2)$ (**1-N$_2$H$_4$**) (eq 1).[19] The origin of this unusual reactivity stems from the "imido-like" ground state of **1-N$_2$**, arising from overlap of an out-of-phase linear combination of zirconocene $1a_1$ molecular orbitals with the N_2 π^* system.[20] This key back-bonding interaction is a result of the twisted dimeric structure of **1-N$_2$**, where a dihedral angle of 65.3° is observed for the angle formed between the planes defined by the zirconium and the two cyclopentadienyl centroids. Isotopic labeling studies are consistent with a mechanism involving 1,2-addition of dihydrogen. This approach has recently been extended to include N_2 functionalization by terminal alkynes.[21]

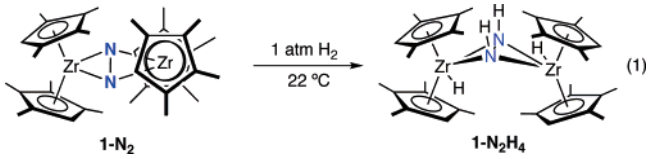

(1)

One open mechanistic question concerning the hydrogenation of **1-N$_2$** is the relative rates of the two hydrogen addition steps (eq 2). While both isotopic labeling experiments and the thermal rearrangement of **1-N$_2$H$_4$** have provided evidence for the product of a single hydrogen addition, $[(\eta^5\text{-}C_5Me_4H)_2ZrH][(\eta^5\text{-}C_5Me_4H)_2Zr](\mu_2,\eta^2,\eta^2\text{-}NNH)$ (**1-N$_2$H$_2$**), this intermediate has yet to be detected directly. In this contribution, the first kinetic measurements on the hydrogenation of coordinated dinitrogen for a series of side-on bound zirconocene dinitrogen complexes are described, and the kinetic isotope effects for H_2 versus D_2 addition have been measured. An unusual dinitrogen functionalization by 1,2-addition of a saturated carbon−hydrogen bond is also described, reinforcing the significance of the imido-like character of the ground states of twisted, side-on bound zirconocene dinitrogen complexes.

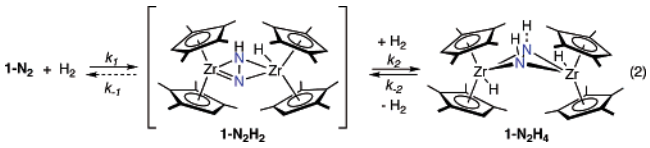

(2)

Results and Discussion

Synthesis, Characterization, and Hydrogenation of Side-On Bound Zirconocene Dinitrogen Complexes. To provide additional experimental support for the importance of the imido-like character in zirconocene dinitrogen complexes for the addition of dihydrogen, new side-on bound N_2 compounds with twisted ground-state structures were targeted. Special care must be taken when designing molecules of this type given the sensitivity of the hapticity of the dinitrogen ligand to the size and number of cyclopentadienyl substituents.[22] If the groups are too large, as in $[(\eta^5\text{-}C_5Me_5)_2Zr(\eta^1\text{-}N_2)]_2(\mu_2,\eta^1,\eta^1\text{-}N_2)$[23] and $[(\eta^5\text{-}C_5Me_5)(\eta^5\text{-}C_5Me_4H)Zr(\eta^1\text{-}N_2)]_2(\mu_2,\eta^1,\eta^1\text{-}N_2)$,[20] end-on coordination is observed and loss of free N_2 and formation of the zirconocene dihydride occurs upon H_2 addition. On the basis of these observations, two mixed ring zirconocene dichloride complexes, $(\eta^5\text{-}C_5Me_5)(\eta^5\text{-}C_5H_2\text{-}1,2\text{-}Me_2\text{-}4\text{-}R)ZrCl_2$ (R = Me,[24] **2-Cl$_2$**; Ph, **3-Cl$_2$**), were prepared using standard literature procedures, and their dinitrogen chemistry was explored. We reasoned that alkylated cyclopentadienyl ligands would be sufficiently reducing to allow synthesis of the N_2 complexes by alkali metal reduction. Previous studies from our laboratory have demonstrated that electron-poor zirconocene dihalides undergo partial reduction to the corresponding Zr(III) monohalide upon treatment with excess sodium amalgam.[22,25]

Reduction of **2-Cl$_2$** or **3-Cl$_2$** with an excess of 0.5% sodium amalgam followed by filtration and isolation from pentane at −35 °C afforded the dinitrogen complexes, $[(\eta^5\text{-}C_5Me_5)(\eta^5\text{-}C_5H_2\text{-}1,2\text{-}Me_2\text{-}4\text{-}R)Zr]_2(\mu_2, \eta^2,\eta^2\text{-}N_2)$ (R = Me, **2-N$_2$**; Ph, **3-N$_2$**), as forest green solids in high yield (eq 3). As expected for dimers containing heteroleptic zirconocenes, a mixture of two isomeric dinitrogen complexes was obtained in each case. For **2-N$_2$**, a 1:1.6 ratio of *syn* and *anti* isomers was observed, whereas a similar ratio of 1:1.9 was obtained for **3-N$_2$**. In context of this work, the *syn* descriptor refers to the isomer where the like cyclopentadienyl ligands are adjacent across the dimer and *anti* designates the case where like rings are opposite (eq 3).

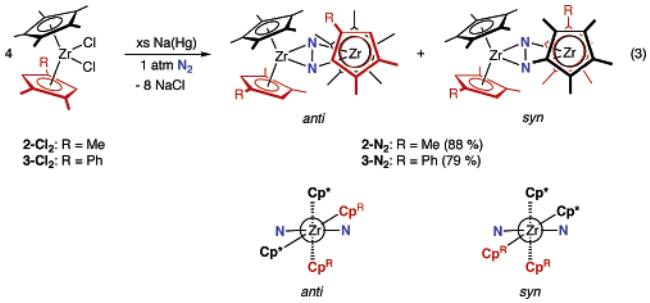

(3)

Characterization of **2-N$_2$** and **3-N$_2$** has been accomplished by a combination of multinuclear (^{1}H, ^{13}C, and ^{15}N) NMR spectroscopy, combustion analysis, and, in the case of **3-N$_2$**, single-crystal X-ray diffraction. Because the spectroscopic

(15) Fryzuk, M. D.; Love, J. B.; Rettig, S. J. *Science* **1997**, *275*, 1445.
(16) Basch, H.; Musaev, D. G.; Morokuma, K.; Fryzuk, M. D.; Love, J. B.; Seidel, W. W.; Albinati, A.; Koetzle, T. F.; Klooster, W. T.; Mason, S. A.; Eckert, J. *J. Am. Chem. Soc.* **1999**, *121*, 523.
(17) Basch, H.; Musaev, D. G.; Morokuma, K. *J. Am. Chem. Soc.* **1999**, *121*, 5754.
(18) Basch, H.; Musaev, D. G.; Morokuma, K. *Organometallics* **2000**, *19*, 3393.
(19) Pool, J. A.; Lobkovsky, E.; Chirik, P. J. *Nature* **2004**, *427*, 527.
(20) Pool, J. A.; Bernskoetter, W. H.; Chirik, P. J. *J. Am. Chem. Soc.* **2004**, *126*, 14326.
(21) Bernskoetter, W. H.; Pool, J. A.; Lobkovsky, E.; Chirik, P. J. *J. Am. Chem. Soc.* **2005**, *127*, 7901.
(22) Pool, J. A.; Chirik, P. J. *Can. J. Chem.* **2005**, *83*, 286.
(23) Manriquez, J. M.; Bercaw, J. E. *J. Am. Chem. Soc.* **1974**, *96*, 6229.
(24) Wolczanski, P. T.; Bercaw, J. E. *Organometallics* **1982**, *1*, 793.

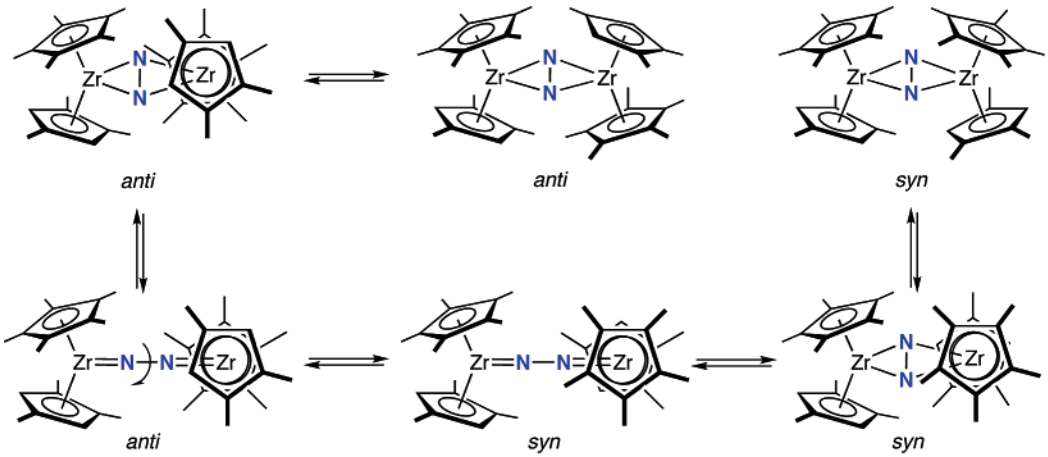

Figure 1. Proposed mechanism for intramolecular dynamics and isomer interconversion in **2-N_2**.

properties of the two compounds are similar, only the data for **2-N_2** will be discussed in detail. The data for **3-N_2** are presented in the Supporting Information. The benzene-d_6 ^{1}H NMR spectrum of **2-N_2** recorded at 23 °C exhibits the number of resonances expected for two isomeric C_2 symmetric zirconocene dinitrogen complexes, where the two halves of the dimer are related by the axis of rotation. For each isomer, three inequivalent methyl groups and two inequivalent cyclopentadienyl hydrogens are observed for the [$C_5Me_3H_2$] ligand, indicating a lack of symmetry about each zirconocene monomer.

To probe the possibility of isomer interconversion in benzene-d_6 solution, a series of EXSY NMR experiments were performed. At 23 °C and a mixing time of 300 ms, two sets of cross-peaks are observed in the major isomer. Under these conditions, no exchange is observed for the minor. In the major, pairwise exchange is observed for two cyclopentadienyl methyl groups and the two cyclopentadienyl hydrogens, establishing a dynamic process that interchanges the two lateral sides of each zirconocene monomer. No exchange between the two isomers was observed at this temperature and mixing time. Warming the sample to 35 °C and increasing the mixing time to 500 ms allowed observation of site exchange in the minor, where cross-peaks are observed for the pairwise exchange for the lateral cyclopentadienyl methyl groups and hydrogens. Further warming to 50 °C again with a 500 ms mixing time produced cross-peaks indicative of exchange between the two isomers. Thus, site exchange within the major and minor isomers occurs with a lower barrier than isomer exchange. It should be noted that exchange between the major and minor isomers appears fast on the chemical time scale as the same distribution of isomers has been consistently observed from different synthetic batches and purification procedures.

Additional information about the symmetry of each isomer in solution has been obtained from the ^{15}N NMR spectrum of **2-N_2**. In benzene-d_6 at 23 °C, three peaks are observed—a singlet centered at 623.53 ppm and two doublets of equal intensity centered at 622.73 and 625.73 ppm, respectively. Both doublets have $^1J_{N-N}$ coupling constants of 22 Hz. Similar spectral features are observed for **3-N_2**, with a singlet centered at 629.47 ppm and two doublets at 623.10 and 631.23 ppm, with 22 Hz $^1J_{N-N}$ coupling constants. These chemical shifts are in excellent agreement with the value of 621.1 ppm observed for **1-N_2**.[19] In both **2-N_2** and **3-N_2**, the singlets are assigned to the *syn* isomer, as this configuration has a C_2 axis that bisects the N−N bond and equivalences the two nitrogen atoms. In the *anti* isomer, the C_2 axis contains the N−N bond and does not relate the two nitrogen atoms but does equivalence the two halves of the dimer. As a result, two ^{15}N NMR resonances are observed with typical $^1J_{N-N}$ coupling constants.[26]

Definitive identification of the major and minor isomers by routine two-dimensional NMR experiments is prohibited by peak overlap and *syn*−*anti* exchange. Despite this limitation, the exchange data provide some circumstantial evidence for isomer assignment. The relatively low barrier to pairwise methyl and cyclopentadienyl hydrogen exchange observed for the major isomer by EXSY NMR spectroscopy can be accounted for by a rocking (twisting) of the dimer, where lateral methyl groups and hydrogens exchange (Figure 1). Because this same process is only observed at higher temperatures with the minor isomer, we tentatively assign the major as the *anti* configuration as eclipsing different cyclopentadienyl rings should be more favorable than eclipsing two [C_5Me_5] ligands in the *syn* case. Conducting the EXSY experiment at 50 °C and with a 500 ms mixing time without additional N_2 present also produced cross-peaks for isomer exchange. These observations suggest that intramolecular rocking accounts for site exchange within each zirconocene, and a side-on, end-on interconversion that does not require N_2 coordination most likely accounts for the isomer exchange (Figure 1).

The phenyl-substituted dinitrogen complex, **3-N_2**, has been further characterized by single-crystal X-ray diffraction. The molecular structure of the compound is presented in Figure 2, and selected bond distances and angles are reported in Table 1. The solid-state structure confirms the identity of the molecule as the side-on bound dinitrogen complex, where the dimer is twisted with a dihedral angle of 72.9° between the planes defined by the zirconium and the cyclopentadienyl centroids. This value is slightly larger than the angle of 65.3° observed for **1-N_2**[19] and may be a result of increased steric congestion about the zirconium center. The N−N bond length of

(25) Pool, J. A.; Lobkovsky, E.; Chirik, P. J. *J. Am. Chem. Soc.* **2004**, *125*, 2241.
(26) Fryzuk, M. D.; Johnson, S. A.; Patrick, B. O.; Albinati, A.; Mason, S. A.; Koetzle, T. F. *J. Am. Chem. Soc.* **2001**, *123*, 3960.

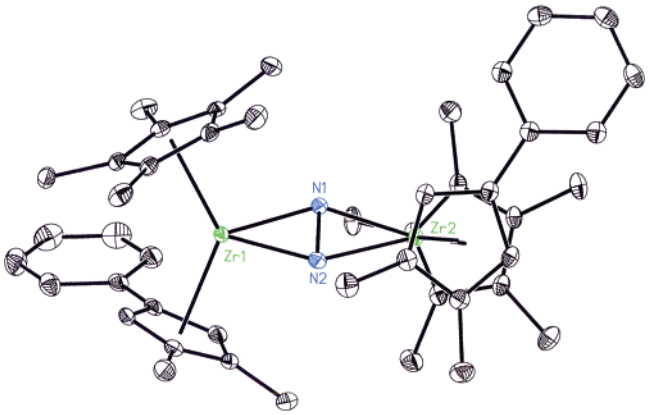

Figure 2. Molecular structure of **3-N$_2$** at 30% probability ellipsoids. Hydrogen atoms omitted for clarity.

Table 1. Selected Bond Distances (Å) and Angles (deg) for **3-N$_2$**

Zr(1)−N(1)	2.1053(14)
Zr(1)−N(2)	2.0845(15)
Zr(2)−N(1)	2.1022(14)
Zr(2)−N(2)	2.0882(15)
N(1)−N(2)	1.3787(19)
N(1)−Zr(1)−N(2)	38.40(5)
N(1)−Zr(2)−N(2)	38.42(5)
N(2)−N(1)−Zr(2)	70.25(9)
N(2)−N(1)−Zr(1)	70.06(9)
N(1)−N(2)−Zr(1)	70.54(9)
Zr(1)−N(1)−Zr(2)	140.19(7)
Zr(1)−N(2)−Zr(2)	142.75(8)
Cp−Zr−Cp[a]	131.2
dihedral angle[b]	72.9

[a] Angle formed between the cyclopentadienyl centroids and the metal center. [b] Angle formed between the planes defined by the zirconium centers and their respective centroids.

1.3787(19) Å is comparable to the value of 1.377(3) Å found in **1-N$_2$**. While the Zr_2N_2 core is essentially planar,[27] the bonding between the zirconium and the nitrogen atoms is asymmetric. Relatively long Zr−N bonds of 2.1053(14) and 2.1022(14) Å are formed to N(1), while shorter distances of 2.0845(15) and 2.0882(14) Å are observed for N(2). Only the *anti* isomer of **2-N$_2$** is observed in the crystal lattice. Analysis of the crystals by ^{1}H NMR spectroscopy in benzene-d_6 revealed the presence of both isomers in approximately a 1:1.9 ratio, consistent with rapid equilibration of the isomers in solution. However, fortuitous crystal selection or selective crystallization cannot be ruled out.

With two new side-on bound zirconocene dinitrogen complexes in hand, their reactivity toward dihydrogen was explored. Addition of 1 atm of H_2 to benzene-d_6 solutions of either **2-N$_2$** or **3-N$_2$** induced a color change from dark green to faint yellow over the course of minutes at 23 °C. The relative rates of disappearance for each isomer are indistinguishable by NMR spectroscopy. This could be a result of nearly identical rates of hydrogenation of the *syn* and *anti* N_2 complexes or rapid equilibration between isomers and selective addition of H_2 to one compound. A combination of multinuclear NMR data, solid-state IR spectroscopy, and combustion analysis identified the products of the hydrogenation as the hydrido zirconocene diazenido complexes, $[(\eta^5\text{-}C_5Me_5)(\eta^5\text{-}C_5H_2\text{-}1,2\text{-}Me_2\text{-}4\text{-}R)ZrH]_2(\mu_2,\eta^2,\eta^2\text{-}N_2H_2)$ (R = Me, **2-N$_2$H$_4$**; Ph, **3-N$_2$H$_4$**; eq 4). Selected spectroscopic features are reported in Table 2. Both isomers of **2-N$_2$H$_4$** and **3-N$_2$H$_4$** exhibit relatively upfield shifted ^{1}H and ^{15}N NMR resonances, indicative of side-on bound diazenido ligands.[21] For **3-^{15}N$_2$H$_4$**, the ^{1}H NMR spectrum displays an AA′XX′ pattern for the N−H resonances. Spectral simulation[28] provided the following coupling constants: $^3J_{H-H} = 13.9$ Hz, $^1J_{N-H} = 57.0$ Hz, $^2J_{N-H} = 0.17$ Hz, and $^1J_{N-N} = 14.0$ Hz, which are similar to those reported in related isotopically labeled acetylido zirconocene diazenido complexes.[21]

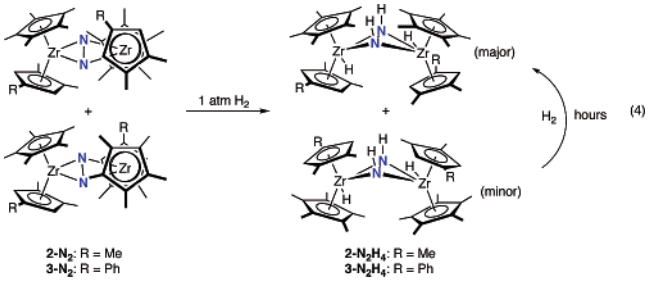

Both the major and minor isomers of **2-N$_2$H$_4$** exhibit C_2 symmetry with one zirconium hydride resonance, one N−H, two cyclopentadienyl hydrogens, and four cyclopentadienyl methyls—one for the $[C_5Me_5]$ ring and three for the $[C_5Me_3H_2]$ ligand. Similar symmetry is observed for **3-N$_2$H$_4$**. These symmetries, along with equivalent zirconium hydrides, suggested that both of the observed isomers are *syn* with *transoid* hydride ligands. Unlike the dinitrogen complexes, the pyramidalization of the diazenido ligand generates two possibilities for the *syn* conformation, where the N−H bonds are directed either toward the $[C_5Me_5]$ rings or toward the $[C_5Me_3H_2]$ ligands. The NOESY spectrum (23 °C, 300 ms mixing time) for the major isomer exhibits cross-peaks between the $[C_5Me_5]$ ring and the N−H resonances, establishing the identity of this isomer as the one in which the N−H bonds are directed toward the $[C_5Me_5]$ ligand. This isomer alleviates the interactions between the sterically demanding $[C_5Me_5]$ rings and is a result of the pyramidalization of the diazenido core. The NMR data also demonstrate that the major and minor isomers of **2-N$_2$H$_4$** do not interconvert on the NMR time scale at 23 °C. However, the major isomer does exhibit broadened resonances at temperatures above −20 °C and is most likely a result of rapid side-on, end-on interconversion of the N_2H_2 ligand, as we have previously reported in related compounds.[21]

Monitoring the hydrogenation of **2-N$_2$** in situ by ^{1}H NMR spectroscopy provides additional information about the relative stability of the isomeric products. Initially a 1:1.5 mixture of two isomers of **2-N$_2$H$_4$** is observed, suggesting that either both isomers of **2-N$_2$** are hydrogenated or one isomer reacts preferentially with H_2 and yields two isomers of the hydrido zirconocene diazenido compound. Continuing the hydrogenation for 4−6 h at 23 °C induces complete conversion of the minor isomer into the major. If the solution is allowed to stand without H_2 present, products arising from loss of 1 equiv of H_2 and subsequent α-migration are observed, in analogy to the reactivity previously reported for **1-N$_2$H$_4$**.[19,20] If the hydrogenation procedure is carried out on a preparative scale for 12 h followed by recrystallization from pentane at −35 °C, only the major isomer is obtained. Similar observations have been made for **3-N$_2$**, and the results of these experiments are presented in the

(27) The deviations from the idealized Zr_2N_2 plane are N(1) and N(2), 0.033 Å; Zr(1), 0.031 Å; Zr(2), 0.21 Å.
(28) Marat, K. *Spinworks*; University of Manitoba: Manitoba, Canada, 2004.

Table 2. Selected Spectral Data for **1-N_2H_4**, **2-N_2H_4**, **3-N_2H_4**, **4**, and **5**

	1-N_2H_4	**2-N_2H_4** (major)	**2-N_2H_4** (minor)	**3-N_2H_4** (major)	**3-N_2H_4** (minor)	**4**	**5**
N−H[a]	0.83	0.71 ppm	1.29 ppm	0.73 ppm	1.23 ppm	1.45 ppm	1.56 ppm
Zr−H[a]	4.51	4.51 ppm	4.73 ppm	4.79 ppm	4.77 ppm		
^{15}N[b]	74.5 ppm	79.08 ppm	102.29 ppm	91.93 ppm		102.51 ppm	105.19 ppm
N−H[c]	3235[d] cm^{-1}	3298 cm^{-1}		3286 cm^{-1}		3301 cm^{-1}	3290 cm^{-1}
Zr−H[c]	1554 cm^{-1}	1531 cm^{-1}		1544 cm^{-1}			

[a] ^{1}H NMR spectrum in benzene-d_6 at 23 °C. [b] ^{15}N NMR chemical shifts recorded in benzene-d_6 at 23 °C relative to liquid ammonia. [c] Frequencies determined from solid-state infrared spectroscopy. [d] Value recorded in benzene solution.

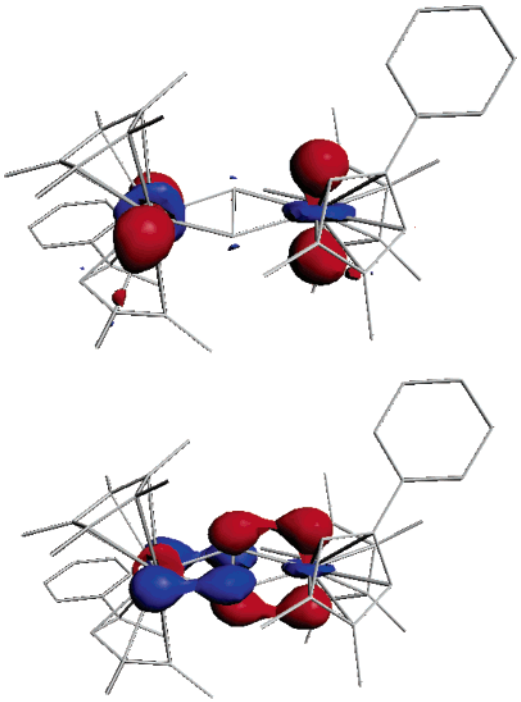

Figure 3. Frontier molecular orbitals of **3-N_2** computed from DFT calculations (ADF2004.01, TZ2P, ZORA). Top: LUMO (−2.123 eV). Bottom: HOMO (−2.826 eV).

Supporting Information. Likely mechanisms for conversion of the minor isomer into the major include inversion of the diazenido nitrogen atoms or a side-on, end-on interconversion of the N_2H_2 core coupled to a Zr−N or N−N bond rotation.

The hydrogenation of the N_2 ligand in both **2-N_2** and **3-N_2** prompted investigation of the electronic structures of these compounds with DFT calculations. A full molecule calculation was conducted (ADF2004.001, TZ2P, ZORA) on **3-N_2** using the coordinates from the solid-state structure as the starting point for the geometry optimization. The computed frontier molecular orbitals of the compound are presented in Figure 3. As was found for **1-N_2**,[20] the HOMO of **3-N_2** is an out-of-phase linear combination of zirconocene $1a_1$ molecular orbitals that overlap with the π^* molecular orbitals of the side-on bound N_2 ligand. The LUMO is the in-phase combination of the zirconocene orbitals and lies approximately 16 kcal/mol higher in energy than the HOMO.

Electronic Spectra of Side-On Bound Zirconocene Dinitrogen Complexes. At typical concentrations used for NMR spectroscopy (~0.02 M), the rates of hydrogenation of the side-on dinitrogen complexes are too fast to obtain reliable kinetic data. Moreover, complications from inefficient gas mixing in an NMR tube confined to a temperature-controlled NMR probe also suggested that other techniques may be more appropriate for making kinetic measurements. Because dramatic color changes from forest green to faint yellow are observed upon dinitrogen hydrogenation, electronic spectroscopy seemed well suited for measuring the rate of H_2 addition.

Before kinetic measurements were made, the electronic spectrum of each dinitrogen complex, **1-N_2**, **2-N_2**, and **3-N_2**, and the corresponding hydrido zirconocene diazenido compounds were recorded in heptane solution. Sample spectra of each N_2 complex are shown in Figure 4, while molar absorptivities (ϵ) and absorption maxima (λ_{max}) are presented in Table 3. The notable feature of each spectrum is the intense (ϵ = 8900−11 400) absorption in the near-infrared region. Considering the frontier molecular orbitals of **1-N_2** and **3-N_2**, these peaks are most likely due to principally ligand-to-metal charge transfer transitions (LMCT), arising from a HOMO comprised of the zirconium−nitrogen back-bond to a LUMO that is essentially pure metal *d*, consisting of a primarily out-of-phase linear combination of zirconocene $1a_1$ orbitals. The absorbance maxima correlate with the carbonyl stretching frequencies, where the most reducing zirconocene dinitrogen complexes with purely alkylated substituents, **1-N_2** and **2-N_2**, contain the lower CO stretching frequencies and more blue shifted LMCT bands relative to the phenyl-substituted compound, **3-N_2**.[29] Significantly, the electronic spectra of **1-N_2H_4**, **2-N_2H_4**, and **3-N_2H_4** are transparent in this region, providing a convenient handle for the measurement of rates of N_2 hydrogenation.

Cooling a heptane solution of **1-N_2** to −78 °C under a N_2 atmosphere produced a color change from forest green to intense purple. A similar phenomenon was observed when the dinitrogen compound was dissolved in benzene or toluene at ambient temperature. The forest green solutions can be maintained by avoiding exposure to N_2 at either low or ambient temperature. Likewise, purple heptane solutions regain their green color upon warming or removal of the N_2 atmosphere. Observation of intense purple solutions is reminiscent of the end-on dinitrogen complexes, $[(\eta^5\text{-}C_5Me_5)(\eta^5\text{-}C_5Me_4R)]Zr(\eta^1\text{-}N_2)]_2(\mu_2,\eta^1,\eta^1\text{-}N_2)$ reported by Bercaw (R = Me)[23] and our laboratory (R = H),[20] and suggests additional N_2 forms the end-on dinitrogen complex, $[(\eta^5\text{-}C_5Me_4H)_2Zr(\eta^1\text{-}N_2)]_2(\mu_2,\eta^1,\eta^1\text{-}N_2)$ (**1-$(N_2)_3$**, eq 5), perhaps due to the increased solubility of N_2 in heptane upon cooling. The −78 °C electronic spectrum of a purple heptane solution of **1-N_2** recorded under an atmosphere of N_2 exhibits three new bands centered at 401, 549, and 667 nm. These peaks are similar to those reported at 392, 544, and 771 nm for $[(\eta^5\text{-}C_5Me_5)_2Zr(\eta^1\text{-}N_2)]_2(\mu_2,\eta^1,\eta^1\text{-}N_2)$.[30] On the basis of the decrease in intensity for the **1-N_2** peak compared to that for the mixture of **1-$(N_2)_3$** and **1-N_2** in equimolar samples, the end-on dinitrogen

(29) Zachmanoglou, C. E.; Docrat, A.; Bridgewater, B. M.; Parkin, G. E.; Brandow, C. G.; Bercaw, J. E.; Jardine, C. N.; Lyall, M.; Green, J. C.; Kiester, J. B. *J. Am. Chem. Soc.* **2002**, *124*, 9525.
(30) Sanner, R. D.; Manriquez, J. M.; Marsh, R. E.; Bercaw, J. E. *J. Am. Chem. Soc.* **1976**, *98*, 8351.

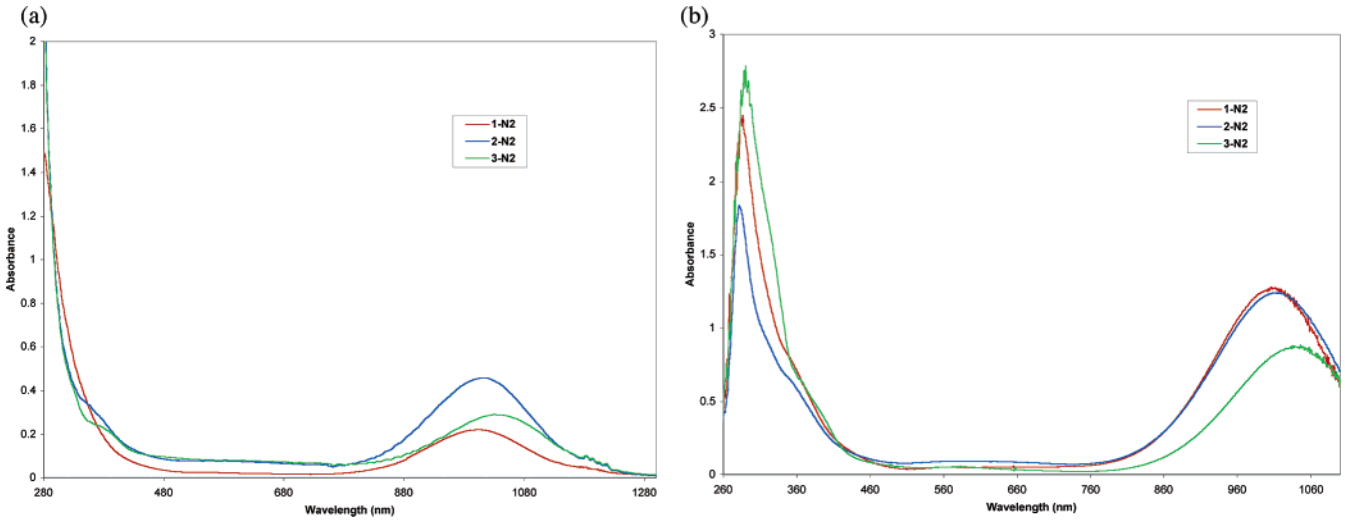

Figure 4. Electronic spectra of **1-N$_2$**, **2-N$_2$**, and **3-N$_2$** in heptane at 23 °C recorded on (a) Shimadzu UV-3101 spectrophotometer and (b) Hewlett-Packard 8543E spectrophotometer.

Table 3. Absorption Maxima (λ_{max}) and Extinction Coefficients (ϵ) for Zirconocene Dinitrogen Complexes Recorded in Heptane Solution

	1-N$_2$		**2-N$_2$**		**3-N$_2$**	
	λ_{max}[a]	ϵ	λ_{max}	ϵ	λ_{max}	ϵ
	280	11700	279	12900	276	13700
	351	3700	363	3400	366	3100
	648		651	460	654	310
	1006	11400	1014	8900	1046	9200
ν(CO)[b]	1951	1858	1951	1858	1952	1860

[a] Values reported in nanometers. [b] CO stretching frequencies of the corresponding zirconocene dicarbonyl complexes recorded in pentane solution.

complex accounts for approximately 10−15% of the zirconocene in solution at −78 °C in heptane.

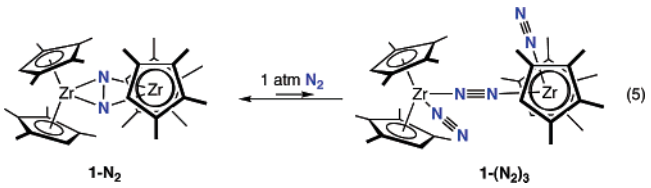

(5)

Additional evidence for the formation of **1-(N$_2$)$_3$** under N_2 was provided by solution infrared spectroscopy. The toluene solution IR spectrum of the mixture of **1-N$_2$** and **1-(N$_2$)$_3$** recorded at 23 °C exhibits two strong peaks centered at 2010 and 2045 cm^{-1}, assigned to the stretches of the terminal N_2 ligands. These values are in good agreement with those reported for [(η^5-C_5Me_5)$_2$-Zr(η^1-N$_2$)]$_2$(μ_2,η^1,η^1-N$_2$) (2006, 2041 cm^{-1})[31] and [(η^5-C_5Me_5)(η^5-C_5Me_4H)Zr(η^1-N$_2$)]$_2$(μ_2,η^1,η^1-N$_2$) (2003, 2046 cm^{-1}).[20] While present in only small amounts, **1-(N$_2$)$_3$** offers distinct spectroscopic (and visual) characteristics diagnostic of its formation.

The observation of **1-(N$_2$)$_3$** in the presence of additional N_2 also provides insight into the mechanism of ^{15}N isotopic exchange in side-on zirconocene dinitrogen compounds. Exposure of a benzene-d_6 solution of **1-N$_2$** to 1 atm of $^{15}N_2$ gas over the course of 24 h at 23 °C furnishes **1-^{15}N$_2$** in greater than 90% isotopic purity. Performing similar procedures with **2-N$_2$** and **3-N$_2$** affords **2-^{15}N$_2$** and **3-^{15}N$_2$**, respectively, although mixing for at least 5 days is required for similar levels of isotopic incorporation. While **2-(N$_2$)$_3$** and **3-(N$_2$)$_3$** have not been directly detected either by electronic or IR spectroscopy upon cooling to −78 °C, isotopic exchange most likely occurs through the end-on intermediates shown in Figure 5. As will be described in greater detail in the next section, the increased steric hindrance imparted by the [C_5Me_5] ligands in **2-N$_2$** and **3-N$_2$** is believed to be the origin of the slower rates of exchange in the heteroleptic zirconocenes.

Kinetics of Dinitrogen Hydrogenation. With a reliable spectroscopic technique in hand, the kinetics of hydrogenation of coordinated dinitrogen were examined. At this point, it is useful to describe the experimental procedure for the determination of rate constants. A more thorough account of the apparatus and setup can be found in the Experimental Section and Supporting Information. In a typical kinetic run, a 0.173 mM stock heptane solution of the desired N_2 complex was charged into a cuvette and a calibrated gas volume attached. The bulb was charged with a large excess of dihydrogen, typically greater than 5000 equiv, and the assembly placed in a temperature-controlled block inside a UV−vis spectrometer. After exposure of the heptane solution to the H_2 gas, the disappearance of the LMCT band for the N_2 complex was monitored as a function of time. Throughout the experiment, the reaction mixture was continuously stirred and the entire temperature block periodically removed and the apparatus thoroughly shaken to ensure efficient mixing of H_2 in solution. Typical kinetic experiments were repeated several times and were reproducible.

For experimental convenience, **2-N$_2$** was selected as the representative N_2 complex for the majority of the kinetic studies. Monitoring the disappearance of the band at 1014 nm as a function of time in the presence of a large excess (>5000 equiv) of H_2 established a pseudo-first-order reaction for the conversion to **2-N$_2$H$_4$**. Plots of concentration versus time for various orders in zirconium are presented in the Supporting Information. To determine the order in dihydrogen, the H_2 pressure was systematically varied while the zirconium concentration was held constant. It should be noted that at pressures less than 0.400 atm, pseudo-first-order kinetics were not maintained and are

(31) Manriquez, J. M.; McAlister, D. R.; Rosenberg, E.; Shiller, A. M.; Williamson, K. L.; Chan, S. I.; Bercaw, J. E. *J. Am. Chem. Soc.* **1978**, *100*, 3078.

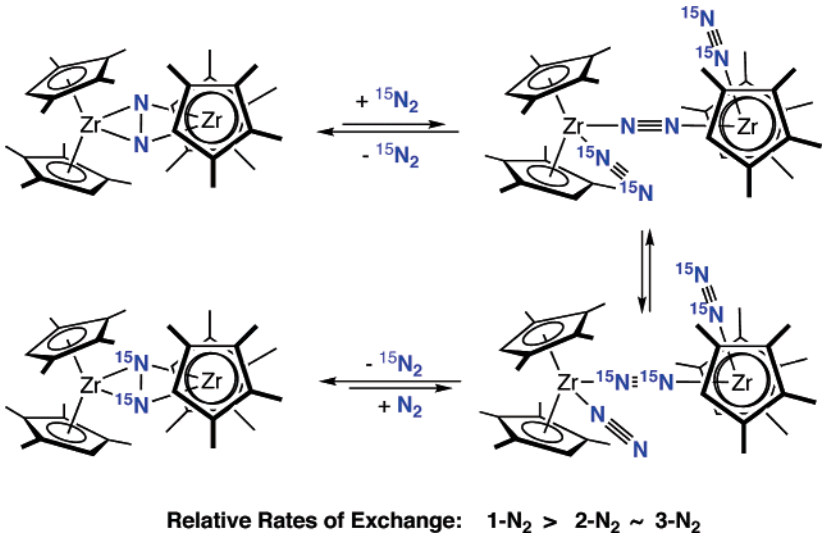

Figure 5. Proposed mechanism for isotopic exchange in zirconocene dinitrogen complexes.

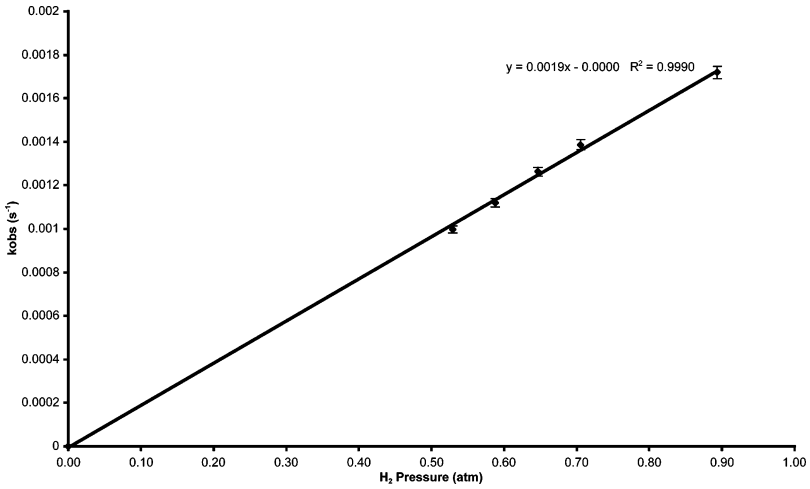

Figure 6. Plot of k_{obs} versus H_2 pressure for determination of order in H_2 for N_2 hydrogenation in **2-N_2**.

Table 4. Observed Rate Constants for the Hydrogenation of **2-N_2** at 23 °C as a Function of Dihydrogen Pressure

H_2 pressure (atm)[a]	$k_{obs} \times 10^3$ (s^{-1})[b]
0.529	0.99(1)
0.588	1.12(1)
0.647	1.26(1)
0.705	1.39(2)
0.894	1.7(2)

[a] Pressure of H_2 charged into a 112.7 mL volume at 23 °C. [b] Runs conducted at 23 °C at 0.173 mM **2-N_2**.

Table 5. Relative Rates of Hydrogenation of N_2 as a Function of Cyclopentadienyl Substituents and Corresponding Kinetic Isotope Effects

compound	k_{obs} (s^{-1})[a]	k_{rel}	KIE
1-N_2	$3.9(4) \times 10^{-3}$	4.1	2.4(2)
2-N_2	$1.2(1) \times 10^{-3}$	1.3	2.2(2)
			2.1(2)[b]
3-N_2	$9.5(1) \times 10^{-4}$	1.0	1.8(3)

[a] Determined at 0.647 atm of H_2 at 23 °C. [b] Determined by ^{1}H NMR spectroscopy.

most likely a result of diffusion-limited mixing of the H_2 gas with the heptane solution.

The experimentally determined pseudo-first-order rate constants as a function of dihydrogen pressure are presented in Table 4, and a plot of observed rate constant versus pressure is contained in Figure 6. The linear fit ($R^2 = 0.999$) to the data clearly establishes a first-order dependence on H_2 addition and an overall second-order process for dinitrogen hydrogenation (eq 6).

$$\text{Rate} = k_1[\textbf{2-N}_2][H_2] \quad (6)$$

The relative rates of hydrogenation for the other side-on bound zirconocene dinitrogen complexes were also measured. The pseudo-first-order rate constants collected at 0.647 atm of H_2 are reported in Table 5. As expected for zirconocenes with similar steric environments reacting with a small molecule such as dihydrogen, the substituent effects are modest. The most sterically hindered complex, **3-N_2**, hydrogenates the slowest, while the more open homoleptic complex, **1-N_2**, reacts only slightly faster (~4 times). Interestingly, the rates of hydrogenation parallel the qualitative rates for $^{15}N_2$ isotopic exchange, where **2-N_2** and **3-N_2** undergo approximately the same (slower) rate of isotopic enrichment, while $^{15}N_2$ incorporation for **1-N_2** is relatively facile.

The activation parameters for dinitrogen hydrogenation were determined by measuring the rate constants for the addition of

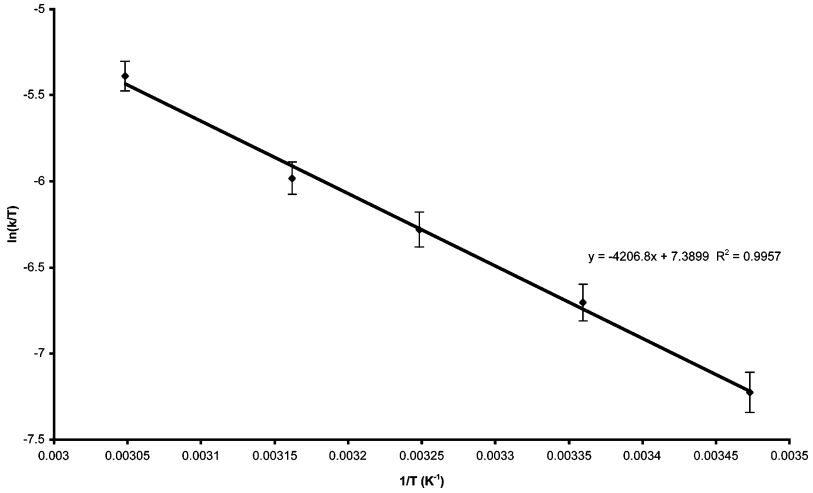

Figure 7. Eyring plot for the hydrogenation of **2-N_2**.

H_2 to **2-N_2** over a 40 °C temperature range. For these experiments, it is assumed that H_2 is an ideal gas and forms an ideal solution when dissolved in heptane. The concentration of dissolved gas as a function of temperature was determined from literature data.[32] An Eyring plot (Figure 7) was constructed from five rate constants and yielded activation parameters of $\Delta H^{\ddagger} =$ 8.4(8) kcal/mol and $\Delta S^{\ddagger} = -33(4)$ eu. An entropy of activation of this direction and magnitude is consistent with a bimolecular reaction with an ordered transition structure, consistent with a 1,2-addition of H_2. This value is in agreement with the $\Delta S^{\ddagger}$ of -35 eu that has been reported for the σ-bond metathesis of styrene with $(\eta^5\text{-}C_5Me_5)_2ScMe$, which proceeds through a similar four-centered transition structure.[33]

Kinetic isotope effects were also measured for the hydrogenation (deuteration) of coordinated dinitrogen to provide additional mechanistic information (Table 5). Experimental determination of k_H/k_D was accomplished by comparing the observed pseudo-first-order rate constants obtained at 23 °C for H_2 versus D_2 addition. In each case, normal, primary kinetic isotope effects are observed and are consistent with H−H bond breaking in the rate-determining step of N_2 hydrogenation. For **2-N_2**, the value of 2.2(1) determined from UV−vis data was independently confirmed using NMR spectroscopy, which yielded a statistically identical kinetic isotope effect of 2.1(1).[34] The latter determination was carried out by measuring the conversion of **2-N_2** in parallel NMR experiments in the presence of either H_2 or D_2 for fixed time intervals.

The kinetic data, in combination with the kinetic isotope effects and activation parameters, present a fairly complete picture of N_2 hydrogenation in side-on bound zirconocene dinitrogen complexes. The observed first-order dependence on H_2 concentration coupled with normal, primary isotope effects and large negative entropies of activation is consistent with the first H_2 addition being rate determining, proceeding through an ordered transition structure where H−H bond scission is simultaneous with Zr−H and N−H bond formation (Figure 8). This transition structure is similar to that proposed for the 1,2-addition of carbon−hydrogen bonds to group 4 imido complexes. In these compounds, both experimental[35] and computational[36] studies implicate a planar, four-centered transition structure involving concerted bond breaking and formation with little charge buildup.

Observation of the first H_2 addition as the rate-determining step in the hydrogenation of coordinated N_2 is also in agreement with computational studies by Morokuma on the hydrogenation of $[(p_2n_2)Zr]_2(\mu_2,\eta^2,\eta^2\text{-}N_2)$.[16,17] In this case, the calculations support a concerted addition pathway where H−H bond scission is simultaneous with N−H and Zr−H bond formation. An activation barrier of 21.6 kcal/mol was computed for the hydrogenation of bis(phosphine)bis(amido) zirconium dinitrogen complexes and is good agreement with the experimental observation of a slower (∼1 week, 23 °C) hydrogenation reaction. By comparison, the bis(cyclopentadienyl)zirconium dinitrogen complexes offer lower experimentally determined barriers for H_2 addition, on the order of 18 kcal/mol, and may be a consequence of a reduced steric environment, although the electronic variations imparted by the different ancillary ligands cannot be excluded.

Dinitrogen Functionalization by 1,2-Addition of Saturated Carbon−Hydrogen Bonds. Gently warming toluene or benzene solutions of **2-N_2** or **3-N_2** to 65 °C over the course of 2 days resulted in smooth conversion of the dinitrogen compounds to the cyclometalated zirconocene diazenido complexes, $[(\eta^5\text{-}C_5Me_5)(\eta^5\text{-}C_5H_2\text{-}2\text{-}Me\text{-}4\text{-}R\text{-}1\text{-}\eta^1\text{-}CH_2)Zr]_2(\mu_2,\eta^2,\eta^2\text{-}N_2H_2)$ (R = Me, **4**; Ph, **5**). These products are a result of formal 1,2-addition of a carbon−hydrogen bond followed by alkyl migration (eq 7). Both **4** and **5** have been characterized by a combination of multinuclear NMR spectroscopy, infrared spectroscopy, combustion analysis, and X-ray diffraction. In each case, only one isomer of the cyclometalated zirconocene diazenido complex is observed.

Selected spectroscopic features for both complexes are contained in Table 2. For both compounds, N−H resonances are observed by ^{1}H NMR spectroscopy at 1.45 and 1.56 ppm

(32) *Solubility Data Series*, 1st ed.; Young, C. L., Ed.; International Union of Pure and Applied Chemistry; Vol 5.
(33) Thompson, M. E.; Baxter, S. M.; Bulls, A. R.; Burger, B. J.; Nolan, M. C.; Santarsiero, B. D.; Schaefer, W. P.; Bercaw, J. E. *J. Am. Chem. Soc.* **1987**, *109*, 203.
(34) For a discussion of kinetic isotope effects for the addition of H_2 and D_2 to transition metal complexes, see: Collman, J. P.; Hegedus, L. S.; Norton, J. R.; Finke, R. G. *Principles and Applications of Organotransition Metal Chemistry*; University Science Books: Mill Valley, CA, 1987; pp 286−288.
(35) (a) Wolczanski, P. T.; Bennett, J. L. *J. Am. Chem. Soc.* **1997**, *119*, 10696. (b) Wolczanski, P. T.; Bennett, J. L. *J. Am. Chem. Soc.* **1994**, *116*, 2179.
(36) Cundari, T. R.; Klinckman, T. R.; Wolczanski, P. T. *J. Am. Chem. Soc.* **2002**, *124*, 1481.

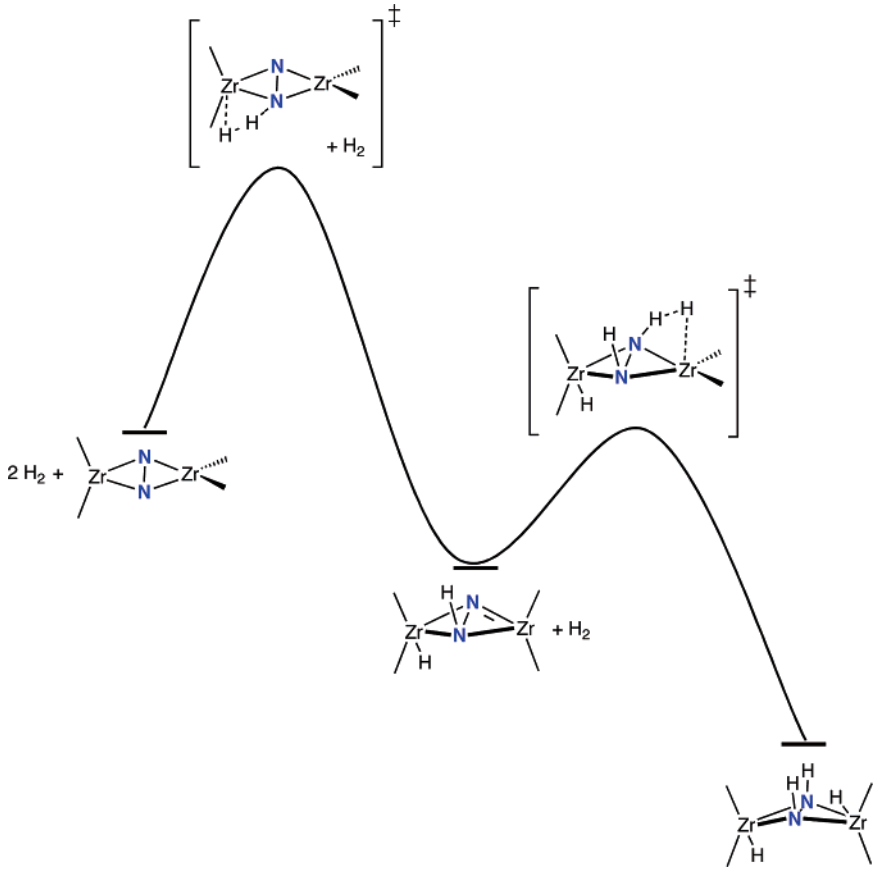

Figure 8. Reaction profile for the hydrogenation of N_2 promoted by zirconocene dinitrogen complexes.

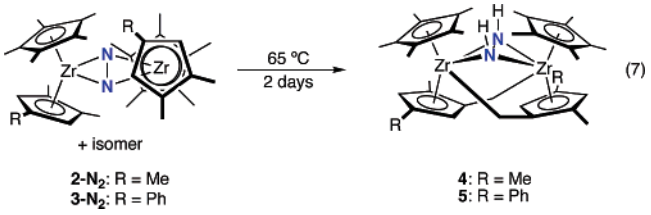

2-N_2: R = Me
3-N_2: R = Ph

4: R = Me
5: R = Ph

(7)

and are diagnostic of a side-on bound diazenido ligand in solution.[21] These peaks split into an AA′XX′ pattern upon labeling with thermolysis of **2-$^{15}N_2$** and **3-$^{15}N_2$**. In addition, relatively upfield shifted ^{15}N NMR resonances are observed at 102.51 and 105.19 ppm, respectively, and are consistent with η^2,η^2 coordination of the N_2H_2 ligand. For **4**, the methylene hydrogens bound to the cyclometalated carbons are observed by ^1H NMR spectroscopy as a doublet of doublets centered at 0.85 ($^2J_{H-H}$ = 9.4 Hz) and 1.64 ($^2J_{H-H}$ = 9.4 Hz). Similar peaks centered at 1.09 ($^2J_{H-H}$ = 9.4 Hz) and 1.97 ($^2J_{H-H}$ = 9.4 Hz) are seen for **5**.

The solid-state structures of both **4** and **5** have been determined by X-ray diffraction and are presented in Figures 9 and 10, respectively. The crystals of **5** contained a molecule of pentane in the lattice, but it has been omitted for clarity in Figure 10. Selected metrical parameters are reported in Table 6. For **5**, the data were of sufficient quality such that the hydrogens attached to nitrogen were located in the Fourier difference map and refined. Unfortunately, this was not the case for **4**. However, on the basis of the solution NMR data, solid-state infrared spectroscopy, and the observed pyramidalization about the nitrogens in the crystal structure, we are confident of N−H bond formation. In both structures, only one isomer is observed with

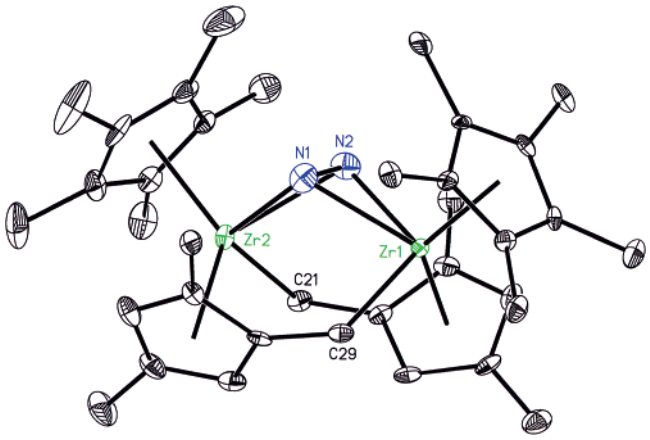

Figure 9. Molecular structure of **4** at 30% probability ellipsoids.

a side-on bound diazenido ligand and the N−H bonds directed toward the sterically demanding [C_5Me_5] ligands. These conformations are similar to those proposed for the major isomers of the hydrido zirconocene diazenido compounds and are believed to be a result of reduced steric interactions between the relatively large [C_5Me_5] ligands. Interestingly, the solid-state structures reveal cyclometalation *across* the zirconocene diazenido dimer, arising from formal 1,2-addition of a cyclopentadienyl methyl C−H bond followed by alkyl migration (vide infra). In both complexes, cyclometalation of the analogous methyl group of the [C_5H_2-1,2-Me_2-4-R] ring is observed.

The bond distances and angles in **4** and **5** are similar to those reported for other zirconocene diazenido complexes.[19,21] Typical N−N bond distances of 1.435(7) and 1.433(3) Å are observed,

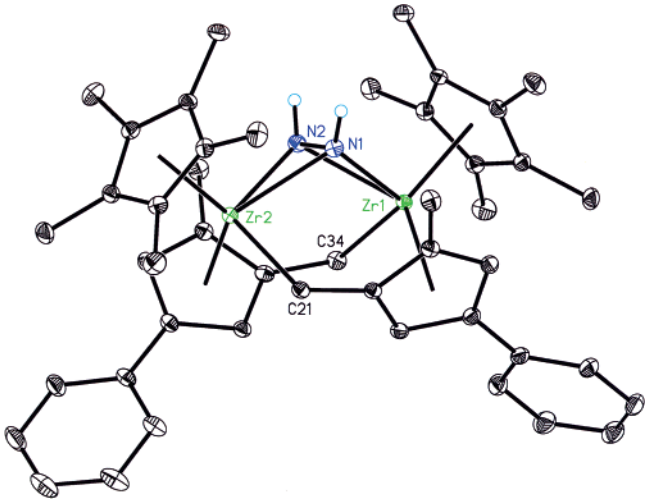

Figure 10. Molecular structure of **5** at 30% probability ellipsoids. Hydrogen atoms, except for those attached to nitrogen, and co-crystallized pentane molecule omitted for clarity.

Table 6. Selected Bond Distances (Å) and Angles (deg) for **4** and **5**

	4	5
Zr(1)−N(1)	2.316(5)	2.1478(19)
Zr(1)−N(2)	2.118(5)	2.3353(19)
Zr(2)−N(1)	2.151(6)	2.3733(19)
Zr(2)−N(2)	2.387(5)	2.1453(18)
N(1)−N(2)	1.435(7)	1.433(3)
N(1)−Zr(1)−N(2)	37.44(18)	36.98(7)
N(1)−Zr(2)−N(2)	36.41(18)	36.53(7)
N(2)−N(1)−Zr(1)	63.7(3)	78.64(11)
N(2)−N(1)−Zr(2)	80.8(3)	63.04(10)
N(1)−N(2)−Zr(1)	78.8(3)	64.38(10)
N(1)−N(2)−Zr(2)	62.8(3)	80.42(11)
Zr(1)−N(1)−Zr(2)	103.5(2)	101.99(7)
Zr(1)−N(2)−Zr(2)	102.1(2)	103.31(8)
Cp−Zr−Cp[a]	132.0	131.2

[a] Angle formed between the cyclopentadienyl centroids and the metal center.

and the Zr_2N_2 diazenido core is distorted with relatively short Zr−N distances for the formally "X-type" interactions and longer Zr−N bonds for the "L-types" (Table 6).[37] Both complexes are significantly twisted with dihedral angles of 89.8 and 87.0°, respectively, formed between the planes defined by the zirconiums and the cyclopentadienyl centroids. The cores of the molecules are also more puckered than other crystallographically characterized zirconocene diazenido compounds with 69.9(2) and 70.13(9)° angles between the planes formed between each zirconium and the two nitrogen atoms of the diazenido ligand. For comparison, this value is 46.51(8)° in **1-N_2H_4**[19] and 45.54(5)° in $[(\eta^5\text{-}C_5Me_4H)_2Zr(C{\equiv}C^tBu)]_2(\mu_2,\eta^2,\eta^2\text{-}N_2H_2)$.[21] The larger pucker in both **4** and **5** is a direct consequence of cyclometalation, in which the diazenido core bends substantially to accommodate the proximity of the activated cyclopentadienyl ring.

The activation of a saturated carbon−hydrogen bond by a side-on bound zirconocene dinitrogen complex reinforces the notion of the zirconium−nitrogen multiple bond character in the ground states of these molecules. Both isolated[38] and in situ generated[39] zirconium imido complexes have been shown to activate carbon−hydrogen bonds in solution. Formation of **4** and **5** from the corresponding dinitrogen compounds most likely proceeds by initial C−H activation of a cyclopentadienyl methyl group to yield the intramolecular cyclometalated product where the η^1-methylene is bound to the same zirconium as the η^5-cyclopentadienyl. Evidence for this behavior has been obtained in studying isotopic exchange reactions with **1-N_2D_4** with dihydrogen, where deuteration of the cyclopentadienyl methyl groups is observed upon standing in benzene-d_6 solution. For **4** and **5**, the alkyl rearrangement following intramolecular C−H activation may render the reaction irreversible.

Concluding Remarks

The first experimental measure of the kinetics of the hydrogenation of coordinated dinitrogen has been obtained. Both the order in H_2 and the observation of a normal, primary kinetic isotope effect support rate-determining addition of the first equivalent of dihydrogen. For the limited series of side-on bound zirconocene dinitrogen complexes studied, the cyclopentadienyl substituent effects on H_2 addition are relatively modest. Kinetic isotope effects and the entropy of activation suggest an ordered, four-centered transition structure with synchronous H−H cleavage concomitant with Zr−H and N−H bond formation. The imido-like character of the side-on bound zirconocene dinitrogen complexes is also effective in promoting dinitrogen functionalization by 1,2-addition of a saturated carbon−hydrogen bond, as addition of a cyclopentadienyl methyl group is observed upon mild thermolysis.

Experimental Section[40]

Preparation of $[(\eta^5\text{-}C_5Me_5)(\eta^5\text{-}C_5H_2\text{-}1,2,4\text{-}Me_3)Zr]_2(\mu_2,\eta^2,\eta^2\text{-}N_2)$ (2-N_2). A 20 mL scintillation vial was charged with 14.25 g of 0.5% sodium amalgam and 5 mL of toluene. With vigorous stirring of the amalgam, a slurry of 0.250 g (0.618 mmol) of $(\eta^5\text{-}C_5Me_5)(\eta^5\text{-}C_5H_2\text{-}1,2,4\text{-}Me_3)ZrCl_2$ in 5 mL of toluene was added. The resulting reaction mixture was stirred for 3 days at ambient temperature under a dinitrogen atmosphere, turning royal blue after 1 day, then changing to dark green over the next 2 days. Following filtration through Celite, the solvent was removed in vacuo, leaving a dark green solid, which was washed with 20 mL of pentane to yield 0.189 g (88%) of dark green solid, observed as a 1:1.6 mixture of two isomers by ^{1}H NMR spectroscopy. Anal. Calcd for $C_{36}H_{52}Zr_2N_2$: C, 62.19; H, 7.54; N, 4.03. Found: C, 62.08; H, 7.90; N, 3.86. **Major Isomer**: ^{1}H NMR (benzene-d_6, 23 °C) δ = 1.96 (s, 30H, C_5Me_5), 1.98 (s, 6H, $C_5Me_3H_2$), 2.05 (s, 6H, $C_5Me_3H_2$), 2.21 (s, 6H, $C_5Me_3H_2$), 5.20 (d, 2H, 2.8 Hz, $C_5Me_3H_2$), 5.34 (d, 2H, 2.8 Hz, $C_5Me_3H_2$). $\{^1H\}^{13}$C NMR (benzene-d_6, 23 °C): δ = 12.51, 12.63, 13.67, 14.21 (Cp*Me*), 110.66, 111.19 (Cp). **Minor Isomer**: ^{1}H NMR (benzene-d_6, 23 °C) δ = 1.97 (s, 30H, C_5Me_5), 1.98 (s, 6H, $C_5Me_3H_2$), 2.00 (s, 6H, $C_5Me_3H_2$), 2.18 (s, 6H, $C_5Me_3H_2$), 5.19 (d, 2H, 2.8 Hz, $C_5Me_3H_2$), 5.35 (d, 2H, 2.8 Hz, $C_5Me_3H_2$). $\{^1H\}^{13}$C NMR (benzene-d_6, 23 °C): δ = 12.56, 12.63, 14.08, 14.42 (Cp*Me*), 108.83, 110.10 (Cp). **Combined Isomers:** $\{^1H\}^{15}$N NMR (benzene-d_6, 23 °C): δ = 622.72 (d, 22 Hz), 623.53 (s), 625.73 (d, 22 Hz).

Preparation of $[(\eta^5\text{-}C_5Me_5)(\eta^5\text{-}1,2,4\text{-}C_5Me_3H_2)ZrH]_2(\mu_2,\eta^2,\eta^2\text{-}N_2H_2)$ (2-N_2H_4). A thick-walled glass reaction vessel was charged with 0.100 g (0.144 mmol) of **2-N_2**, and 20 mL of toluene was added. On a high vacuum line, the vessel was submerged in liquid nitrogen and 1 atm of dihydrogen admitted. The contents of the vessel were warmed

(37) For a description of the "L" and "X" formalism, see: Green, M. L. H. *J. Organomet. Chem.* **1995**, *500*, 127.

(38) Hoyt, H. M.; Michael, F. E.; Bergman, R. G. *J. Am. Chem. Soc.* **2004**, *126*, 1018.

(39) Schaller, C. P.; Cummins, C. C.; Wolczanski, P. T. *J. Am. Chem. Soc.* **1996**, *118*, 591.

(40) General considerations and additional experimental procedures can be found in the Supporting Information.

to ambient temperature, and the resulting reaction mixture was stirred for 12 h, forming a pale red solution. The solvent and excess H_2 were removed in vacuo, and the solid was recrystallized from pentane at −35 °C to yield 0.043 g (42%) of an off-white powder identified as **2-N_2H_4**. Following this procedure, only the major isomer is observed. The minor isomer may be observed from the in situ hydrogenation of **2-N_2** in benzene-d_6. Anal. Calcd for $C_{36}H_{54}Zr_2N_2$: C, 61.83; H, 8.07; N, 4.01. Found: C, 62.09; H, 8.33; N, 3.87. **Major Isomer**: ^{1}H NMR (benzene-d_6, 23 °C) $\delta = 0.71$ (s, 2H, N-*H*), 1.89 (s, 30H, C_5Me_5), 2.05 (bs, 6H, $C_5Me_3H_2$), 2.33 (bs, 6H, $C_5Me_3H_2$), 2.52 (bs, 6H, $C_5Me_3H_2$), 4.51 (s, 2H, Zr-*H*), 5.32 (bs, 2H, $C_5Me_3H_2$), 5.63 (bs, 2H, $C_5Me_3H_2$). ^{1}H NMR (benzene-d_6, 40 °C): $\delta = 0.73$ (s, 2H, N-*H*), 1.92 (s, 30H, C_5Me_5), 2.06 (bs, 6H, $C_5Me_3H_2$), 2.31 (bs, 6H, $C_5Me_3H_2$), 2.47 (bs, 6H, $C_5Me_3H_2$), 4.49 (s, 2H, Zr-*H*), 5.30 (bs, 2H, $C_5Me_3H_2$), 5.46 (bs, 2H, $C_5Me_3H_2$). ^{1}H NMR (toluene-d_8, −40 °C): $\delta = 0.73$ (s, 2H, N-*H*), 1.88 (s, 30H, C_5Me_5), 2.01 (s, 6H, $C_5Me_3H_2$), 2.28 (s, 6H, $C_5Me_3H_2$), 2.62 (s, 6H, $C_5Me_3H_2$), 4.42 (s, 2H, Zr-*H*), 5.23 (bs, 2H, $C_5Me_3H_2$), 5.63 (bs, 2H, $C_5Me_3H_2$). $\{^1H\}^{13}$C NMR (benzene-d_6, 23 °C): $\delta = 13.16$, 13.93, 16.51 (Cp*Me*), 107.85, 112.28, 114.45 (Cp). $\{^1H\}^{15}$N NMR (benzene-d_6, 23 °C): $\delta = 79.08$. IR (KBr): $\nu_{N-H} = 3298$ cm^{-1}, $\nu_{Zr-H} = 1531$ cm^{-1}, $\nu_{Zr-D} = 1101$ cm^{-1}. **Minor Isomer**: ^{1}H NMR (benzene-d_6, 23 °C) $\delta = 1.29$ (bs, 2H, N-*H*), 1.93 (s, 30H, C_5Me_5), 2.18 (s, 6H, $C_5Me_3H_2$), 2.27 (bs, 6H, $C_5Me_3H_2$), 2.37 (bs, 6H, $C_5Me_3H_2$), 4.73 (s, 2H, Zr-*H*), 4.99 (bs, 2H, $C_5Me_3H_2$), 5.11 (bs, 2H, $C_5Me_3H_2$). $\{^1H\}^{15}$N NMR (benzene-d_6, 23 °C): $\delta = 102.29$.

Preparation of [(η^5-C_5Me_5)(η^5-C_5H_2-2,4-Me_2-1-η^1-CH_2)Zr]$_2$-(μ_2,η^2,η^2-N_2H_2) (4). A thick-walled glass reaction vessel was charged with 0.067 g (0.096 mmol) of **2-N_2**, and 20 mL of toluene was added. The resulting green solution was heated at 65 °C for 2 days, forming a brown reaction mixture. The solvent was removed in vacuo and the resulting powder recrystallized from a mixture of diethyl ether−pentane at −35 °C, affording 0.041 g (61%) of **4** as dark brown blocks. This procedure also produced crystals suitable for X-ray diffraction. Anal. Calcd for $C_{36}H_{52}N_2Zr_2$: C, 62.19; H, 7.54; N, 4.03. Found: C, 62.78; H, 7.50; N, 4.13. ^{1}H NMR (benzene-d_6, 23 °C): $\delta = 0.85$ (d, 2H, 9.4 Hz, Zr-C*H*$_2$), 1.45 (s, 2H, N-*H*), 1.64 (d, 2H, 9.4 Hz, Zr-C*H*$_2$), 1.74 (s, 30H, C_5Me_5), 1.81 (s, 6H, $C_5Me_2(\mu\text{-}CH_2)H_2$), 2.00 (s, 6H, $C_5Me_2(\mu\text{-}CH_2)H_2$), 5.40 (d, 2H, 2.4 Hz, $C_5Me_2(\mu\text{-}CH_2)H_2$), 5.82 (d, 2H, 2.4 Hz, $C_5Me_2(\mu\text{-}CH_2)H_2$). $\{^1H\}^{13}$C NMR (benzene-d_6, 23 °C): $\delta = 11.91$, 13.97, 14.40 (Cp*Me*), 24.97 (Zr-*C*H$_2$), 107.26, 110.62, 110.85, 113.28, 116.09, 119.13 (Cp). $\{^1H\}^{15}$N NMR (benzene-d_6, 23 °C): $\delta = 102.51$. IR (KBr): $\nu_{N-H} = 3301$ cm^{-1}.

General Procedure for Kinetic Determinations. Using a calibrated pipet, 2.50 mL of a 0.173 mM stock solution of the desired dinitrogen complex in heptane was transferred to the cuvette/gas bulb apparatus described below. The liquid sample was chilled to −78 °C, degassed on a high vacuum line, and the desired pressure of dihydrogen was admitted to the calibrated bulb portion of the apparatus. The bulb was sealed to the atmosphere and from the liquid sample, and the apparatus was inserted into the spectrophotometer and equilibrated to temperature. The lower valve was opened, exposing the reaction mixture to the H_2. Spectra were recorded at 30, 60, or 120 s intervals over approximately 2 half-lives (15−45 min). The sample was shaken vigorously and stirred between recording spectra. The decay of the absorbance at the desired wavelength was converted to concentration (corrected for background absorbance) and fitted to pseudo-first-order plots of ln[Zr_2N_2] versus time, which gave observed rate constants as the slope.

Description of Spectrophotometer Cell. A standard rectangular 10 mm path length cell with a 14/20 ground joint was fitted to the bottom of a calibrated gas bulb (100.7 mL). The gas bulb was built with a 14/20 ground joint on bottom for attachment of the cuvette, a bulb isolated on top and bottom by Teflon valves, and a 24/40 ground joint on top for attachment to a high vacuum line. The volume of the entire apparatus (bottom of cuvette to top Teflon valve) was measured as 112.7 mL.

Acknowledgment. We thank the Department of Energy, Office of Basic Energy Sciences (DE-FG02-05ER659), and the National Science Foundation (CAREER Award to P.J.C.) for financial support. P.J.C. is a Cottrell Scholar sponsored by the Research Corporation and a David and Lucile Packard Fellow in Science and Engineering. We also thank Tom McCarrick for valuable assistance with electronic spectroscopy, and Professor Barry Carpenter for helpful discussions. Cambridge Isotope Laboratories is also acknowledged for a generous gift of $^{15}N_2$.

Supporting Information Available: Additional experimental procedures, selected electronic spectra, kinetic data, and structural data for **3-N_2**, **4**, and **5**. This material is available free of charge via the Internet at http://pubs.acs.org.

JA0538841